Functional characterization of linear delay Langevin equations

Adrián A. Budini[1] and Manuel O. Cáceres[2]

[1]*Max Planck Institute for the Physics of Complex Systems, Nöthnitzer Strasse 38, 01187 Dresden, Germany*
[2]*Centro Atómico Bariloche, Instituto Balseiro, CNEA, Universidad Nacional de Cuyo and CONICET, Avenida E. Bustillo km 9.5,*
8400 Bariloche, Argentina

We present an exact functional characterization of linear delay Langevin equations driven by any noise structure defined through its characteristic functional. This method relies on the possibility of finding an explicitly analytical expression for each realization of the delayed stochastic process in terms of those of the driving noise. General properties of the transient dissipative dynamics are analyzed. The corresponding interplay with a color Gaussian noise is presented. As a full application of our functional method we study a model for population growth with non-Gaussian fluctuations: the Gompertz model driven by multiplicative white shot noise.

I. INTRODUCTION

Since the pioneering work of Langevin, stochastic differential equations [1,2] have become a powerful tool for the study of systems where fluctuations play a fundamental role. The basic idea of this approach consists in adding explicitly random elements in the proper system evolution, and then to characterize the statistical properties of the nonequilibrium dynamics by averaging the evolution over a set of noise realizations. For physical systems provided with a thermodynamical equilibrium state, fluctuation and dissipation appear in a linked way as demanded by the fluctuation dissipation theorem [3]. Except for this situation, fluctuations and dissipation can be considered as independent elements, whose characteristics depend on each particular physical situation. Thus, the fluctuations in general may be non-Gaussian and the dissipative dynamics introduces arbitrary correlation effects or memory contributions.

Memory effects can be rigorously derived by using projector operator techniques [4–7]. This method applies for linear subsystems embedded in a bigger one. Nevertheless, in general it is not possible to use this procedure, and the memory contributions follows from a phenomenological description. In fact, in many natural and physical situations, the memory effects arise as a consequence of an intrinsic delay mechanism, which implies that the dissipative evolution depends on the state of the system in a shifted previous time. Remarkable examples of this situation arise in physics, biology, physiology, etc. [8–18]. This particular signature in the dissipative dynamics motivated the study of differential delay equations [19,20] and delay Langevin equations. An exact analytic treatment of these equations is in general extremely difficult. Nevertheless, some progress was achieved in the characterization of linear stochastic evolutions [21–31] driven by Gaussian fluctuations. One of the goals of the present paper is to go, in this analysis, beyond the Gaussian fluctuations.

As was previously mentioned, non-Gaussian fluctuation appears in a natural way in many situations of interest. Thus, the characterization of linear delay Langevin equations in the presence of any kind of fluctuations is of great value. We note that independently of the type of fluctuations, a linear delay Langevin equation is inherently a non-Markovian process.

The study of non-Markovian Langevin equations have received a lot of attention [32–40]. From a rigorous point of view, these equations can only be completely characterized after knowing the full Kolmogorov hierarchy [1,2], i.e., any n-joint probability, or equivalently any n-time correlation. All this information is encoded in the characteristic functional [1,2] of the process. In fact, this object allows one to get the n-characteristic function of the process, from which any n-joint probability follows from an inverse Fourier transform, and any n-time moment or cumulant follow from an n-derivative operation.

In a set of previous works [41–43] we have presented a procedure to get the characteristic functional of processes defined by linear stochastic Langevin equations with local and nonlocal dissipation. Then, this procedure can also be applied in the present context. Functional techniques have also been introduced by other authors for studying disordered systems [44,45] and stochastic equations with multiplicative noise [46].

In this paper we will apply our functional technique to study the transient and stationary properties of linear delay Langevin equations driven by arbitrary noises defined through their characteristic functional. The basic idea consists in obtaining an explicit expression for the realizations of the delay stochastic process in terms of the dissipative delay Green function, and then to get the characteristic functional of the stochastic process, in terms of that of the driving noise. As a full application, we will characterize the Gompertz growth model [29,30] driven by non-Gaussian fluctuations.

The paper is organized as follows. In Sec. II we review the functional method for the characterization of memorylike Langevin equations. In Sec. III we obtain the Green function corresponding to the linear delay evolution. Then the different dynamical behaviors of this function are analyzed. The interplay between the delay dissipation and a color Gaussian noise is presented. In Sec. IV we apply our formalism to characterize the distributions associated to the Gompertz

model of population growth driven by white shot noise. In Sec. V we give the conclusions.

II. FUNCTIONAL CHARACTERIZATION OF GENERALIZED LINEAR LANGEVIN EQUATIONS

In a previous work [43] we have presented a functional method to characterize equations of the form

$$\frac{d}{dt}u(t) = -\int_0^t dt' \, \Phi(t-t')u(t') + \xi(t). \quad (1)$$

Our method relies in knowing the characteristic functional of the noise

$$G_\xi([k(t)]) = \left\langle \exp i \int_0^\infty dt \, k(t)\xi(t) \right\rangle, \quad (2)$$

where $k(t)$ is an arbitrary test function, $\langle \cdots \rangle$ means an average over noise realizations, and the knowledge of the Green function of the dissipative dynamics corresponding to the evolution (1). Thus, for each realization of the noise, we can express the process $u(t)$ as

$$u(t) = \langle u(t) \rangle_0 + \int_0^t dt' \, \Lambda(t-t')\xi(t'), \quad (3)$$

where $\Lambda(t)$ is the dissipative Green function, and we have defined

$$\langle u(t) \rangle_0 = \Lambda(t)u(0). \quad (4)$$

With these elements, we have demonstrated that the characteristic functional of the process $u(t)$

$$G_u([k(t)]) = \left\langle \exp i \int_0^\infty dt \, k(t)u(t) \right\rangle, \quad (5)$$

can be written as

$$G_u([k(t)]) = G_{\langle u \rangle_0}([k(t)])G_\xi([z(t)]), \quad (6)$$

where

$$G_{\langle u \rangle_0}([k(t)]) = \exp\left\{ i \int_0^\infty dt \, k(t)\langle u(t) \rangle_0 \right\}, \quad (7)$$

and the function $z(t)$ is defined as

$$z(t) = \int_t^\infty dt' \, k(t')\Lambda(t'-t). \quad (8)$$

These results follow after inserting Eq. (3) in the definition Eq. (5) and reordering the order of the time integrals.

We remark that the characteristic functional allows us to characterize in a complete form the non-Markovian process $u(t)$. In fact, any n-joint probability distribution $P(\{u_j,t_j\}_{j=1}^n) \equiv P_n(u_1,t_1;u_2,t_2;\ldots;u_n,t_n)$ can be obtained by inverse Fourier transform of the characteristic function $G_u^{(n)}(\{k_j,t_j\}_{j=1}^n)$ as

$$P(\{u_j,t_j\}_{j=1}^n) = \frac{1}{(2\pi)^n} \int dk_1 \cdots \int dk_n$$

$$\times \exp\left(-i\sum_{j=1}^n k_j u_j \right) G_u^{(n)}(\{k_j,t_j\}_{j=1}^n). \quad (9)$$

The n-characteristic function $G_u^{(n)}(\{k_j,t_j\}_{j=1}^n)$ follows from

$$G_u^{(n)}(\{k_j,t_j\}_{j=1}^n) = G_u([k_\delta(t)]), \quad (10)$$

where the function $k_\delta(t)$ must be taken as

$$k_\delta(t) = k_1\delta(t-t_1) + \cdots + k_n\delta(t-t_n). \quad (11)$$

Thus, using these last two equations and Eqs. (6)–(8), we get

$$G_u^{(n)}(\{k_j,t_j\}_{j=1}^n) = \exp\left\{ i\sum_{j=1}^n k_j\langle u(t_j) \rangle_0 \right\} G_\xi([y(t)]), \quad (12)$$

where the function $y(t)$ reads

$$y(t) = \sum_{j=1}^n \Theta(t_j-t)k_j\Lambda(t_j-t). \quad (13)$$

On the other hand, any n-time moments can be calculated by differentiation of the n-characteristic function as

$$\langle u(t_1)u(t_2)\cdots u(t_n) \rangle = (-i)^n \left. \frac{\partial^n G_u^{(n)}(\{u_j,t_j\}_{j=1}^n)}{\partial k_1 \partial k_2 \cdots \partial k_n} \right|_{k_j=0}. \quad (14)$$

In the next section, we will apply this method to characterize linear delay Langevin equations driven by arbitrary noise structures.

Stationary spectral properties. In general, for arbitrary noise and arbitrary memory kernels, it is not possible to guarantee that the dynamics (1) converges to a stationary state. Nevertheless, if a stationary state exists, it must be independent of the initial condition. Thus, a necessary condition to reach a stationary state is

$$\lim_{t\to\infty}\Lambda(t) \to 0. \quad (15)$$

In addition to this condition, clearly a stationary state can arise only if the driving noise is stationary:

$$\langle \xi(\omega)\xi*(\omega') \rangle = \delta(\omega-\omega')S_\xi(\omega). \quad (16)$$

Here, $\xi(\omega)$ represents the noise in a Fourier domain and $S_\xi(\omega)$ is its power spectrum. By assuming that the process $u(t)$ converges to a stationary state,

$$\langle u(\omega)u*(\omega') \rangle = \delta(\omega-\omega')S_u(\omega), \quad (17)$$

from Eq. (1) it is simple to express the power spectrum $S_u(\omega)$ of the process $u(t)$ as

$$S_u(\omega) = S_\xi(\omega)|\Lambda(\omega)|^2. \quad (18)$$

This formula allows us to characterize the spectral properties of the stationary process in terms of the noise power spectrum and the Fourier transform $\Lambda(\omega)$ of the dissipative Green function.

III. DELAY LANGEVIN EQUATIONS

Delay Langevin equations are a special case of the evolution Eq. (1). By assuming the kernel

$$\Phi(t) = a\ \delta(t) - b\ \delta(t - T), \qquad (19)$$

where, a and b are real constants, the stochastic evolution results in

$$\frac{d}{dt}u(t) = -au(t) + bu(t - T) + \xi(t). \qquad (20)$$

The particularity of this equation comes from the delayed contribution $u(t-T)$. Unlike usual differential equations, delayed equations must be supplied with an initial value function

$$u(t) = \varphi(t), \ t \in [-T, 0]. \qquad (21)$$

The interval $[-T, 0]$ is called preinterval and $\varphi(t)$ is called the prefunction. Due to this functional dependence, the treatment of the averaged evolution is a little different when compared with those corresponding to nondelayed kernels [43]. As we will show, in the present case the Green function that propagates the noise is different from that corresponding to the mean value.

By denoting the Laplace transform as $\tilde{f}(s) = \int_0^\infty dt\ e^{-st}f(t)$, from Eq. (20) we get

$$s\tilde{u}(s) - u(0) = -a\tilde{u}(s) + be^{-sT}[\tilde{u}(s) + \varphi(s,T)] + \tilde{\xi}(s), \qquad (22)$$

where we have used

$$\int_0^\infty dt\ e^{-st}u(t - T) = e^{-sT}[\tilde{u}(s) + \varphi(s,T)]. \qquad (23)$$

Here, the function $\varphi(s,T)$ is defined by

$$\varphi(s,T) \equiv \int_{-T}^0 dt\ e^{-st}\varphi(t). \qquad (24)$$

From Eq. (22), the solution of Eq. (20), for each realization of the noise, reads

$$u(t) = \langle u(t)\rangle_0 + \int_0^t dt'\ \Lambda(t - t')\xi(t'). \qquad (25)$$

This expression will allow us to apply the previously obtained results for the characteristic functional of $u(t)$. Here, the function $\langle u(t)\rangle_0$ is defined through its Laplace transform as

$$\langle \tilde{u}(s)\rangle_0 = \frac{u(0) + be^{-sT}\varphi(s,T)}{s + a - be^{-sT}}. \qquad (26)$$

By using Eq. (23), this last expression is equivalent to the deterministic delay differential equation

$$\frac{d}{dt}\langle u(t)\rangle_0 = -a\langle u(t)\rangle_0 + b\langle u(t - T)\rangle_0, \qquad (27)$$

solved with the initial condition

$$\langle u(t)\rangle_0 = \varphi(t), \ t \in [-T, 0]. \qquad (28)$$

On the other hand, the Laplace transform of the Green function $\Lambda(t)$ is

$$\tilde{\Lambda}(s) = \frac{1}{(s + a - be^{-sT})}. \qquad (29)$$

This expression is equivalent to the evolution

$$\frac{d}{dt}\Lambda(t) = -a\Lambda(t) + b\Lambda(t - T), \qquad (30)$$

with the initial conditions

$$\Lambda(t) = 0, \ t \in [-T, 0) \quad \text{and} \quad \Lambda(0) = 1. \qquad (31)$$

Thus, all information about the prefunction $\varphi(t)$ is carried out by the average $\langle u(t)\rangle_0$. In fact, notice that the Green function satisfies the same equation as $\langle u(t)\rangle_0$, but it must be solved with the null prefunction.

A. Delay Green function

In order to apply our functional formalism, we need an explicit expression for the delay Green function $\Lambda(t)$. This function was first derived in Ref. [21]. Here, in order to clarify the procedure, we present a deduction by using a similar technique. First, by proposing a solution of the form

$$\Lambda(t) = e^{-at}\overline{\Lambda}(t), \qquad (32)$$

from Eq. (30), the function $\overline{\Lambda}(t)$ evolves as

$$\frac{d}{dt}\overline{\Lambda}(t) = b * \overline{\Lambda}(t - T). \qquad (33)$$

Here, the renormalized constant $b*$ reads

$$b* = be^{aT}. \qquad (34)$$

Note that $\overline{\Lambda}(t)$ corresponds to the delay Green function of Eq. (30) in the case $a = 0$. In order to solve Eq. (33), we propose the following ansatz:

$$\overline{\Lambda}(t) = \sum_{m=0}^\infty \overline{\Lambda}^{(m)}(t), \qquad (35)$$

where the functions $\overline{\Lambda}^{(m)}(t)$ are non-null only in the time interval $mT \leq t \leq (m+1)T$. Thus, the evolution of the set of functions $\overline{\Lambda}^{(m)}(t)$ results in

$$\frac{d}{dt}\overline{\Lambda}^{(m)}(t) = b * \overline{\Lambda}^{(m-1)}(t - T). \qquad (36)$$

This infinite set of equations can immediately be integrated as

$$\overline{\Lambda}^{(m)}(t) = \overline{\Lambda}^{(m-1)}(mT) + b * \int_{mT}^t dt'\ \overline{\Lambda}^{(m-1)}(t' - T). \qquad (37)$$

The first term of this expression follows from the boundary condition at the initial time of each interval, i.e., $\overline{\Lambda}^{(m)}(mT) = \overline{\Lambda}^{(m-1)}(mT)$. Taking into account that $\overline{\Lambda}^{(0)}(t) = 1$, the hierar-

chy of equations (37) can be solved iteratively. For the m function $\overline{\Lambda}^{(m)}(t)$, we get

$$\overline{\Lambda}^{(m)}(t) = \sum_{n=0}^{m} \frac{(b*)^n}{n!}(t-nT)^n. \tag{38}$$

Inserting this solution in Eq. (35), and after noting that m is the integer part of (t/T), we get to the compact solution

$$\overline{\Lambda}(t) = \sum_{n=0}^{\text{Int}(t/T)} \frac{(b*)^n}{n!}(t-nT)^n, \tag{39}$$

where Int$(\cdots)$ denotes the integer part. Thus, the Green function Eq. (32) finally results

$$\Lambda(t) = \sum_{n=0}^{\text{Int}(t/T)} \left(\frac{b}{a}\right)^n \frac{e^{-a(t-nT)}}{n!}[a(t-nT)]^n. \tag{40}$$

This expression gives us the desired delay Green function as a sum of shifted Poisson functions $[e^{-at}(at)^n/n!]$ weighted by the dimensionless parameter (b/a) to the power n. Note that the number of terms in this sum increases linearly in time with a rate $1/T$.

By construction $\Lambda(t)$ is a continuous function. On the other hand, it is simple to realize that at times $t=nT$, the nth derivative of the Green function is discontinuous. In contrast, any other derivative is continuous. As we will see explicitly below, these properties imply that for longer times the Green function becomes more and more smooth.

Inserting the solution (40) in Eq. (25), and after some algebra, the solution for each noise's realization can be written in the alternative way

$$u(t) = \langle u(t) \rangle_0 + \sum_{n=0}^{\text{Int}(t/T)} \left(\frac{b}{a}\right)^n \int_0^{t-nT} dt'$$
$$\times \frac{e^{-a(t-nT-t')}}{n!}[a(t-nT-t')]^n \, \xi(t'). \tag{41}$$

This expression can also be obtained by iteratively integrating Eq. (20).

B. Stationary spectrum

As we will see in the next subsection, there is a set of parameter values in the space (a,b,T) that guarantee the condition (15). In this case, for stationary noises, the associated stochastic process to the delay Langevin equation (20) reaches a stationary state whose spectral properties can be characterized through Eq. (18). Therefore, using Eq. (29), with $s=-i\omega$, we get

$$S_u(\omega) = \frac{S_\xi(\omega)}{a^2 + b^2 + \omega^2 + 2b\{a\cos[\omega T] + \omega\sin[\omega T]\}}. \tag{42}$$

In the case $a=0$ we recuperate the known expression [27]

$$S_u(\omega) = \frac{S_\xi(\omega)}{b^2 + \omega^2 + 2b\omega\sin[\omega T]}. \tag{43}$$

In the next subsection we will analyze the stability of the Green function, where these results apply.

C. Stability and characteristic behaviors of the transient dissipative dynamics

Here we will analyze different dynamical behaviors of the delay Green function that arise by changing the values of the parameters a, b, and T.

Of special interest are the stability properties, i.e., the characterization of the set of values of the parameters a, b, and T that guarantee $\lim_{t\to\infty}\Lambda(t)=0$. As our expression Eq. (40) is a particular solution of the deterministic delay evolution Eq. (30), the stability analysis of the Green function is equivalent to the stability analysis of that delay evolution equation. It is known [19,20,26,27] that a necessary and sufficient condition for the stability of any solution of Eq. (30) is

$$T < T_c \equiv \frac{\cos^{-1}\left(\frac{a}{b}\right)}{\sqrt{b^2 - a^2}}. \tag{44}$$

This inequality defines the domain of stability, whose boundaries, in the plane (a,b), are given by the line

$$a = b \tag{45}$$

and the curve defined parametrically as

$$a = -w/\tan(wT), \tag{46}$$

$$b = -w/\sin(wT), \tag{47}$$

where for a given T, $wT \in (0,\pi)$; these two boundaries intersect at the point $(-1/T,-1/T)$ (see Fig. 1 in Ref. [26] with $a \to -a$). For the parametric boundary, the variable w can be identified with the frequency of a solution $\exp[iwt]$ of Eq. (30), which implies the relation

$$w = \sqrt{b^2 - a^2}. \tag{48}$$

In the case $a=0$, it is also possible to predict that for $0 > bT > -1/e$ any solution decays monotonously, and for $-1/e > bT > -\pi/2$ any solution develops a time oscillatory decay. Outside these domain, the solutions, for long times, grow indefinitely [27].

In the next figures we will analyze the behavior of the delay Green function in the domain of stability. In Fig. 1 we have plotted some different behaviors by choosing the parameters a and b over the boundaries of stability. In Fig. 1(a), we have chosen the parameters just over the parametric boundary, Eqs. (46) and (47), with $T=1$ and $w=1$, which implies $a=-0.642093$ and $b=-1.1884$. In the first period of time T the Green function is given by $\Lambda(t)=\exp[-at]$. After this first step, we notice that the Green function oscillates in a regular way. This behavior agrees with the previous analysis of stability. Consistently, the frequency of the oscillations
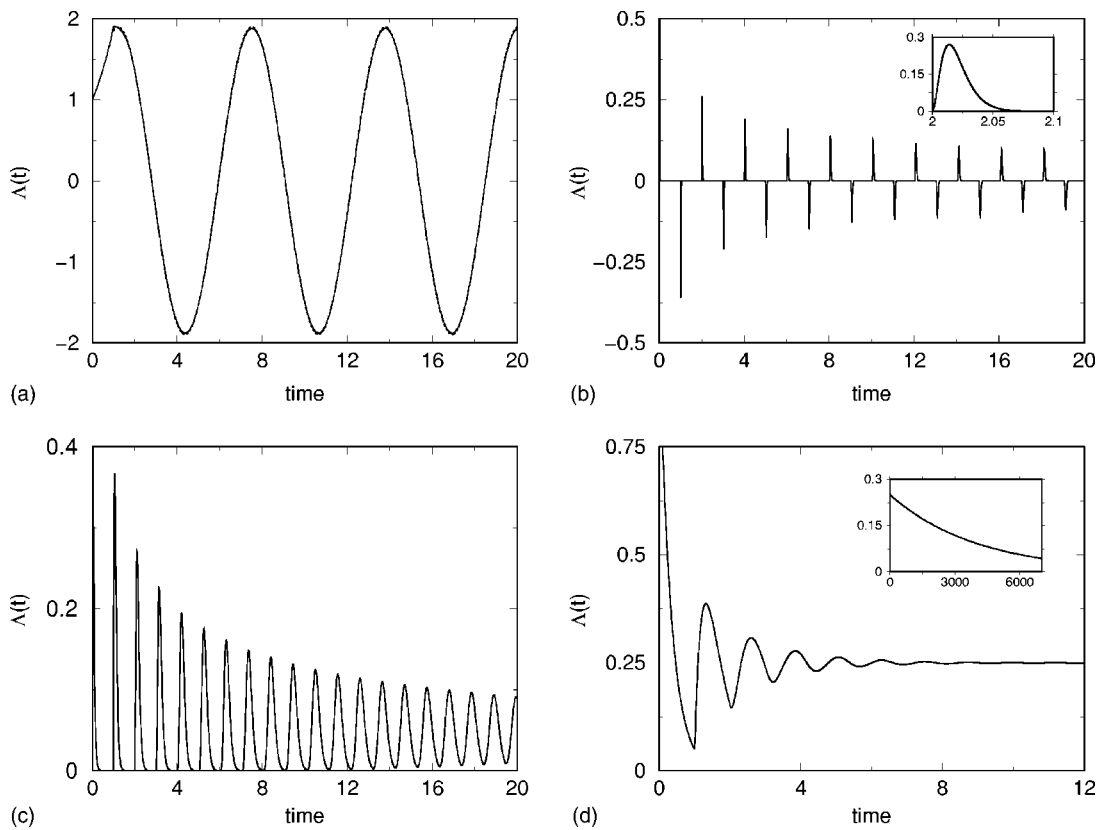
FIG. 1. Delay Green function $\Lambda(t)$ as a function of time in arbitrary units. The parameters are (a) $a=-0.642093$, $b=-1.1884$, values consistent with $w=1$. (b) $a=144.71$, $b=-144.505$, values consistent with $w=3.12$. (c) $a=b=20$, and (d), $a=b=3$; in all cases taking $T=1$.

is given by w. Furthermore, we have checked that after the first interval T, and in the time regime of this plot, $\Lambda(t)$ can be very well adjusted by a trigonometric function (dotted line), $\Lambda(t) \approx A_0 \cos[wt + \phi_0]$, with $A_0 = 1.9$ and $\phi_0 = 0.35$. In general, an analytical adjustment can be only found when the behavior of $\Lambda(t)$ is smooth and regular.

In Fig. 1(b) we have chosen $T=1$, and $w=3.12$ which implies $a=144.71$ and $b=-144.505$. Note that in this case, the dissipative rates $|a|$ and $|b|$ are much larger than $1/T$. In consequence, after a fast exponential decay, the Green function over the first period of time T is approximately zero. At later times, the Green function presents a series of extremely narrow and sharp peaks. In the inset we show the first positive one. We have checked that the period of these oscillating peaks is given by $2\pi/w \approx 2$. As time increases, the pulses become wider and smooth and the Green function becomes more and more smooth. This characteristic arises as a consequence of the continuity of higher derivatives of the Green function as time increases. At even higher times (not showed in the plot), $\Lambda(t)$ becomes an oscillatory function whose behavior can be very well adjusted by a decaying trigonometric function. In general, the rate of this decay is much bigger than the dissipative rates a and b. This slow decay will be analyzed explicitly in the next examples.

When w approaches the value 2π, the absolute value of a and b grows indefinitely. In this situation, the interval over which the Green function presents a narrow behavior also grows. We remark that this unusually sharp behavior implies that the process $u(t)$ will be *closed* most of the time, and will

only respond to the external noise perturbation within narrow windows of time.

In Fig. 1(c) we have chosen the parameters over the other boundary of stability, Eq (45), with $a=b=20$ and $T=1$. The behavior is similar to that of the previous figure. However, in this case the peaks of the Green function are positive at all times. In fact, we have checked that for $b>0$, inside the domain of stability, $\Lambda(t)$ is always positive. We remark that increasing the value of $a=b$, the peaks are narrowed, presenting a structure similar to that of Fig. 1(b).

The main difference of behavior over the two boundaries appears in the long time regime. In fact, the upper boundary of the domain of stability, Eq. (45), can be associated with a solution with frequency $w=0$. Thus, we expect that at long times the Green function becomes a nonoscillatory function. In order to check this change of behavior, in Fig. 1(d) we have chosen $a=b=3$. Here, as the values of the dissipative constants are smaller than in the previous case, only a few peaks appear and the Green function, after a short transient, seems to reach a stationary constant value without any oscillation.

In the inset, we have plotted the Green function for higher values of time. Consistently we found a monotonous decay which can be fitted as $\Lambda(t) \approx A_0 \exp(-\gamma_0 t)$ with $A_0 = 0.25$ and $\gamma_0 = 1/4000$. We notice that the rate of this exponential decay is much less than the dissipative rates a and b. This asymptotic *slowing down decay* is characteristic of the boundaries of stability and it is also present for parameter values near of the boundary line.
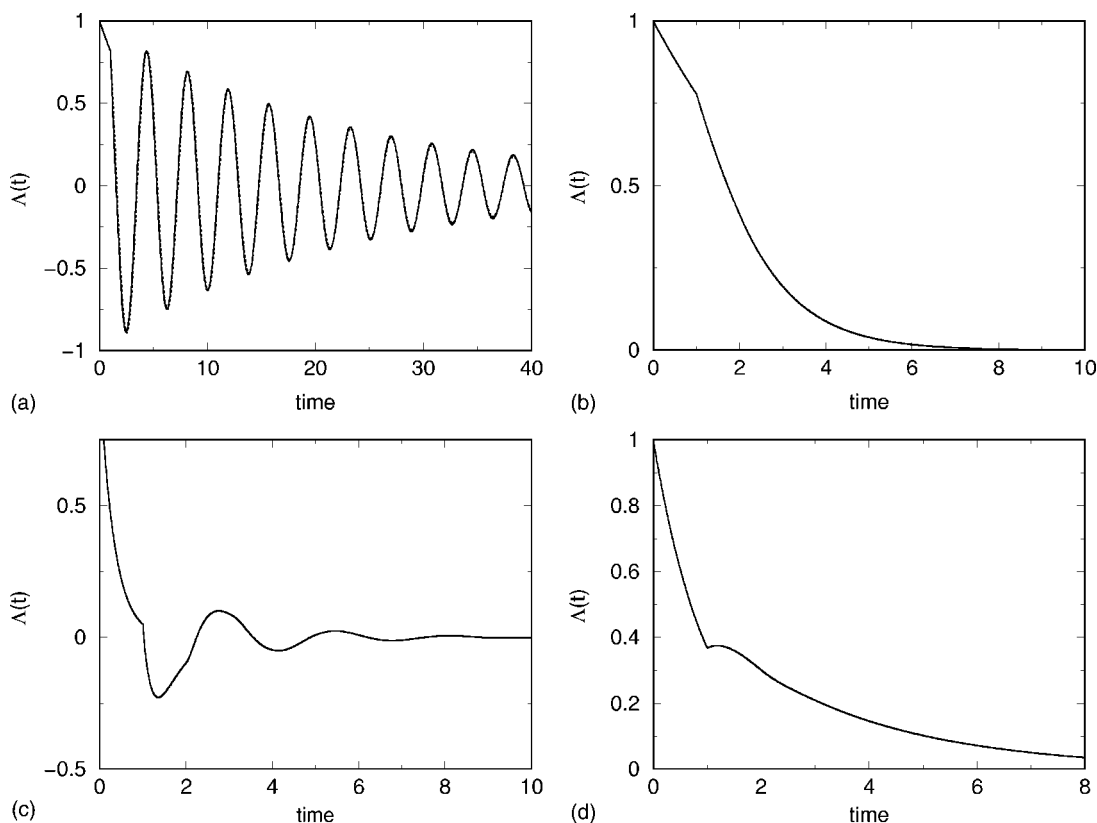
FIG. 2. Delay Green function $\Lambda(t)$ as a function of time in arbitrary units. The parameters are (a), $a=0.2$, $b=-1.6$. (b) $a=25$, $b=-0.25$. (c) $a=3$, $b=-2$. (d) $a=1$, $b=0.45$; in all cases taking $T=1$.

In general, inside the domain of stability, the Green function have different behaviors that approximate the previous analyzed limits. In Fig. 2 we have plotted some of these characteristic behaviors. In Fig. 2(a) we have chosen $a=0.2$, $b=-1.6$, and $T=1$. In this case, the Green function presents a regular and damped oscillatory behavior which, after the first period of time T, can be approximated by $\Lambda(t) \approx A_0 \exp(-\gamma_0 t)\cos(w_0 t + \phi_0)$ (dotted line) with $A_0=1$, $\gamma_0=1/22$, $w_0=1.666$, $\phi_0=1.07$.

In Fig. 2(b), the parameters were chosen as $a=0.25$, $b=-0.25$, and $T=1$. In this case, the Green function can be approximated in a rough way by matching two exponential functions.

In other cases, the Green function does not show a regular behavior, and it is not possible to find a simple analytical approximation valid for all times. Therefore, one can not define a characteristic time scale for the decaying behavior of the Green function. Some examples are shown in Fig. 2(c), where we have chosen $a=3$, $b=-2$, $T=1$ and in Fig. 2(d), where $a=1$, $b=0.45$, and $T=1$.

We remark that in the case $a=0$ the behavior of the Green function is similar to those of Figs. 2(a) and 2(b). In fact, when the local dissipation is zero, after the first step of time, the Green function can be very well adjusted by a monotonous or oscillatory smooth decay. The main difference with the case $a \neq 0$ is the behavior during the first step of time T, where instead of an exponential decay, it takes a constant value $\Lambda(t)=1$.

D. Nonwhite Gaussian noise

Here, we will apply our functional approach to characterize the averaged delay dynamics when the driving noise is a Gaussian one. A zero-mean Gaussian noise $\xi(\tau)$, with an arbitrary correlation function $\sigma_\xi(\tau_2, \tau_1) = \langle \xi(\tau_2)\xi(\tau_1) \rangle$, is characterized by the functional [1]

$$G_\xi([k(t)]) = \exp\left(-\frac{1}{2}\int_0^\infty d\tau_2 \int_0^\infty d\tau_1 \ k(\tau_2)\sigma_\xi(\tau_2, \tau_1)k(\tau_1)\right).$$

$$(49)$$

Therefore, from Eqs. (6)–(8) the characteristic functional of the process $u(t)$ results

$$G_u([k(t)]) = G_{\langle u \rangle_0}([k(t)])$$

$$\times \exp\left(-\frac{1}{2}\int_0^\infty \int_0^\infty d\tau_2 \ d\tau_1 \ k(\tau_2)k(\tau_1)\sigma_u(\tau_2, \tau_1)\right),$$
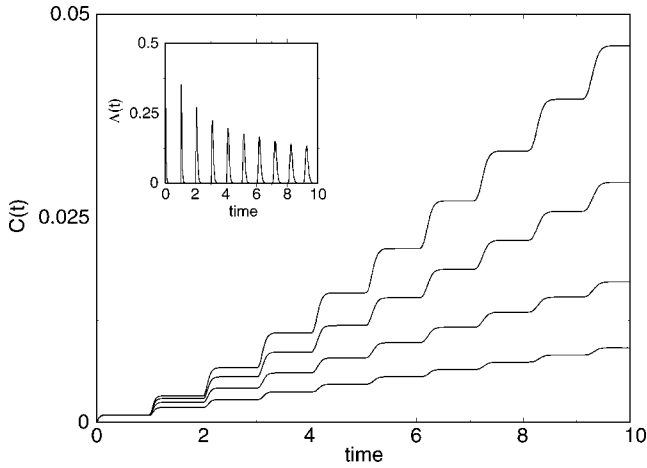
$$(50)$$

where

FIG. 3. Dispersion $C(t)$ of the delay process $u(t)$ driven by a Gaussian noise with an exponential correlation, as a function of time (arbitrary units). The parameters of the Green function (inset) are $T=1$, $a=b=33$. From top to bottom the parameters of the Gaussian color noise are $\gamma=0.25$, 0.5, 1, and 2.5, in all cases taking $B=1$. As initial prefunction we have used the null function.

$$\sigma_u(\tau_2,\tau_1) = \int_0^{\tau_2} dp \int_0^{\tau_1} dq \, \Lambda(\tau_2-p)\sigma_\xi(p,q)\Lambda(\tau_1-q),$$

$$(51)$$

is the correlation function of the process $u(t)$, i.e., $\sigma_u(\tau_2,\tau_1)=\langle u(\tau_2)u(\tau_1)\rangle-\langle u(\tau_2)\rangle\langle u(\tau_1)\rangle$. As expected, the linear delay process $u(t)$ is Gaussian.

Now we will analyze the interplay between the delay dynamics and the noise properties. We will assume an exponential correlation function $\sigma_\xi(\tau_2,\tau_1)=B\exp(-\gamma|\tau_2-\tau_1|)$. Note that in the limit $B\rightarrow\infty$, $\gamma\rightarrow\infty$, with $B/(2\gamma)=D$ this noise reduces to a white Gaussian noise with intensity D.

In the next figures we will describe the averaged dynamics through the quadratic averaged value of $u(t)$

$$C(t) \equiv \langle u^2(t)\rangle - \langle u(t)\rangle^2. \qquad (52)$$

This object can be obtained from Eq. (51) as $C(t)=\sigma_u(t,t)$, with the Green function $\Lambda(t)$ defined by Eq. (40). Of special interest is the transient dynamics over the boundaries of stability. In Fig. 3 we show the behavior of $C(t)$ as a function of time. For the Green function (see inset) we have chosen $a=b=33$ and $T=1$. The different curves correspond to different values of the noise memory parameter. From top to bottom, we have set $\gamma=0.25$, 0.5, 1, and 2.5, in all cases taking $B=1$. As initial condition we have used a null prefunction $\varphi(t)$.

We note that by increasing the noise memory parameter γ, the dispersion of the process $u(t)$ grows with a smaller rate. On the other hand, we note that the growing dynamics have a ladder structure, which is a direct consequence of the peak structure of the Green function $\Lambda(t)$. As expected, in an intermediate regime (not shown in the plot), $C(t)$ loses the ladder structure and in the asymptotic long time regime it reaches a stationary constant value.
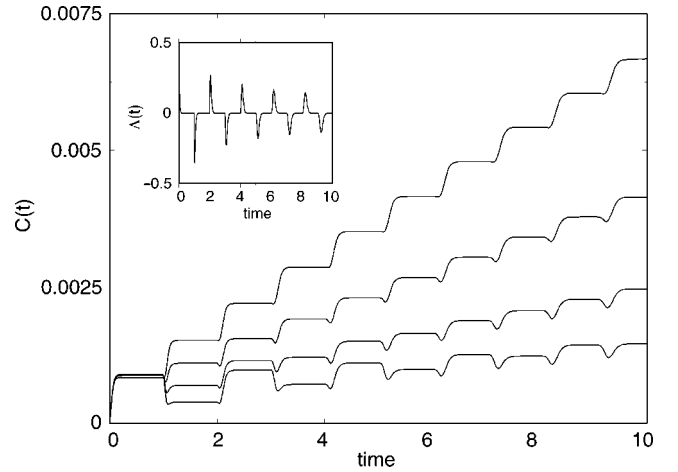

FIG. 4. Dispersion $C(t)$ of the delay process $u(t)$ as in Fig. 3. Here the parameters of the Green function (inset) are $T=1$, $a=33.2064$, $b=33.3462$, which are consistent with $w=3.05$. From bottom to top, the parameters of the Gaussian color noise are $\gamma=0.25$, 0.5, 1, and 2.5, in all cases taking $B=1$.

In Fig. 4 we show the transient behavior of $C(t)$ over the parametric boundary. We have chosen $T=1$ and $w=3.05$, which implies $a=33.2064$ and $b=-33.3462$. In this case, the peaks of the Green function change their sign after each period. From bottom to top we have chosen $\gamma=0.25$, 0.5, 1, and 2.5, in all cases taking $B=1$. In opposition to the previous case, here an increase of the noise memory parameter γ leads to a faster increase of the dispersion $C(t)$. Furthermore, we note that when the characteristic time of the noise memory is bigger than the time step T, i.e., $1/\gamma>T$, during the occurrence of the negative pulses, the dispersion $C(t)$ diminishes.

We remark that the different dependencies of $C(t)$ on the rate γ are directly related with the sign of the Green peaks. On the other hand, in the limit of a white noise, the behavior of $C(t)$ over each boundary is approximately the same. In fact, for the case of δ-correlated Gaussian noise, it is simple to realize that all information of the dissipative dynamics is introduced through the square of the delay Green function $\Lambda^2(t)$ [see Eq. (50) and (51) with $\sigma_u(\tau_2,\tau_1)=D\delta(\tau_2-\tau_1)$].

IV. GOMPERTZ MODEL OF POPULATION GROWTH

In this section we will apply our functional method to characterize a model of population growth with delay. Any realistic model for population dynamics must present two characteristic behaviors. First, for small populations the dynamics must grow in an exponential way; second, a saturation effect must arise in such a way to stop the previous behavior. The delay Gompertz model [29,30] captures all these dynamical properties in a simple way and also takes into account that the growth rate depends on the history of the populations. This nonlinear model reads

$$\frac{dQ(t)}{dt} = bQ(t)\ln\left[\frac{Q(t-T)}{Q^*}\right] + Q(t)\xi(t). \qquad (53)$$

Here, the constant T is related with the maturation or the generation time, the constant Q^* controls the value of the

saturation population, and b scales the exponential growth for small populations. The last term introduces multiplicative fluctuations which are size dependent.

Now we will characterize the average behavior of this model. As it is known [29,30,41], by using the transformation

$$Q(t) = Q * \exp[u(t)], \tag{54}$$

the previous evolution reduces to a linear delay Langevin equation

$$\frac{du(t)}{dt} = bu(t - T) + \xi(t). \tag{55}$$

Thus, the population growth can be completely characterized with our functional approach (Sec. II). First, from the transformation Eq. (54), it is possible to write any n-moment of the population $Q(t)$ as

$$\langle Q(t_1) \cdots Q(t_n) \rangle = Q^{*n} \langle e^{u(t_1)} \cdots e^{u(t_n)} \rangle. \tag{56}$$

The right term of this equality can be expressed in terms of the n-characteristic function of the process $u(t)$. Thus, by using our functional approach, Eq. (12), the n-time moments can finally be expressed in terms of the characteristic functional of the noise $\xi(t)$ as

$$\langle Q(t_1) \cdots Q(t_n) \rangle = Q^{*n} \exp\left\{ \sum_{j=1}^{n} \langle u(t_j) \rangle_0 \right\} G_\xi([g(t)]), \tag{57}$$

where $\langle u(t) \rangle_0$ is defined by Eq. (27) with $a = 0$, and we have introduced the function

$$g(t) = -i \sum_{j=1}^{n} \Theta(t_j - t) \Lambda(t_j - t). \tag{58}$$

The delay Green function $\Lambda(t)$ is given by Eq. (40) after taking $a = 0$.

Also it is possible to obtain any n-joint probability density of the population model. In fact, by using the transformation Eq. (54) any n-joint probability density of $Q(t)$ can be obtained straightforwardly from the relation

$$P(\{Q_j, t_j\}_{j=1}^n) dQ_1 \cdots dQ_n = P(\{u_j, t_j\}_{j=1}^n) du_1 \cdots du_n. \tag{59}$$

Here, any n-joint probability $P(\{u_j, t_j\}_{j=1}^n)$ follows from Eq. (9).

At this point, it is important to remark that the previous results are based in the change of variable Eq. (54). All posteriori calculations were obtained by using a normal derivative calculus. Therefore, in the case of white fluctuations, Eq. (53) must be interpreted as a Stratonovich-Langevin equation [30].

White shot noise

Now we will apply the previous results to the case in which the fluctuations correspond to a symmetrical white shot noise [1,2,41–43]. This noise is defined by the functional
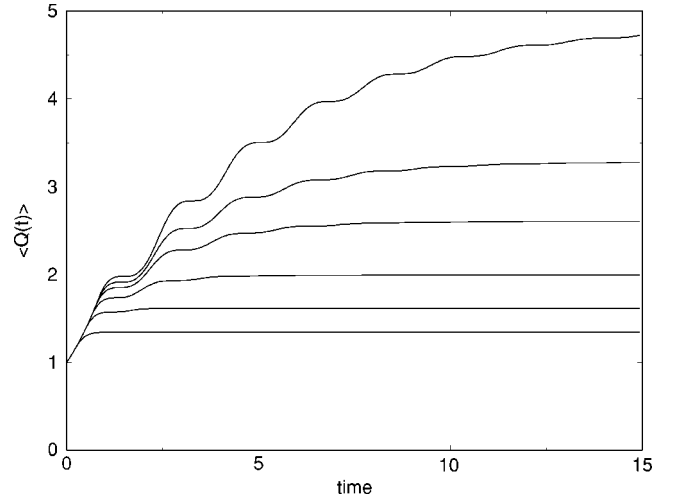

FIG. 5. Average value $\langle Q(t) \rangle$ of the Gompertz model driven by a symmetrical white shot noise. From bottom to top we have chosen $T = 0.25$, 0.5, 0.65, 0.75, 0.8, and 0.85, in all cases taking $b = -\pi/2$. The parameter of the noise are $\rho = 0.15$, $A = \sqrt{1/(2\rho)}$, and the saturation parameter is $Q^* = 1$.

$$G_\xi([k(t)]) = \exp\left(2\rho \int_0^\infty dt \{\cos[Ak(t)] - 1\} \right). \tag{60}$$

The realizations of this noise consist in a series of arriving δ-Dirac peaks with amplitude $\pm A$, where ρ is the density of the arriving pulses in each direction. Notice that in the limit $A \to 0$, $\rho \to \infty$ with $A^2\rho = D/2$, this symmetrical white shot-noise converges to a Gaussian white noise with intensity coefficient D, i.e., Eq. (49) with $\sigma_\xi(\tau_2, \tau_1) = D\delta(\tau_2 - \tau_1)$.

Using Eq. (57), the first moment $\langle Q(t) \rangle$ of the Gompertz model can be written as

$$\langle Q(t) \rangle = Q * \exp\left\{ 2\rho \int_0^t d\tau [\cosh[A\Lambda(\tau)] - 1] \right\}. \tag{61}$$

Here, in order to simplify the analysis we have assumed that the prefunction $\varphi(t)$ of the process $u(t)$ is null, which implies that the prefunction of $Q(t)$ is the constant Q^*. In Fig. 5 we have plotted $\langle Q(t) \rangle$ for different values of the time delay T, maintaining the noise parameters fixed. We found that by increasing T, the saturation value of the process $Q(t)$ increases. In general the behavior of the average value is similar to that found with a Gaussian white noise. Nevertheless, an object that develops strong non-Gaussian characteristics is the one-time probability density.

From Eqs. (12) and (60), for the one-time characteristic function of the process $u(t)$ we get

$$G_u^{(1)}(k, t) = \exp\left\{ 2\rho \int_0^t d\tau \{\cos[Ak\Lambda(\tau)] - 1\} \right\}, \tag{62}$$

where, as in the previous equation, we have assumed that the prefunction of the process $u(t)$ equals zero. This expression allows us to get numerically the one-time probability density at any time by using a fast Fourier algorithm. After, $P(Q, t)$ follows from Eq. (59).
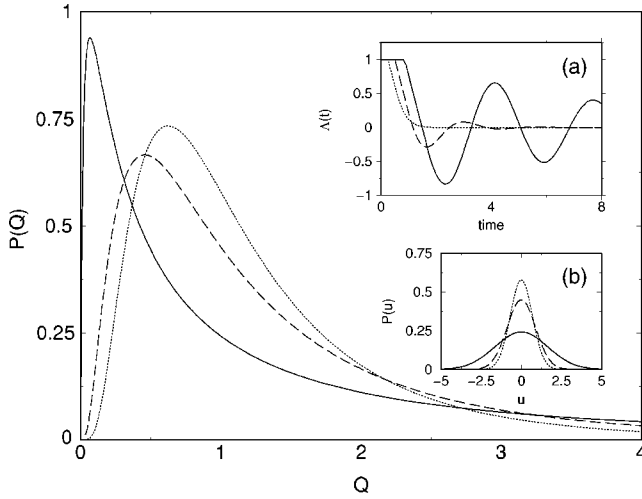
FIG. 6. Stationary distribution $P(Q)$ of the Gompertz model driven by a symmetrical white shot noise for different delay times, $T=0.25$ (dotted line), $T=0.5$ (dashed line), and $T=0.85$ (full line), in all cases taking $b=-\pi/2$. In inset (a) we show the corresponding Green functions $\Lambda(t)$. Inset (b) shows the associated distributions $P(u)$. In all cases, the noise parameters are $\rho=50$ and $A=0.1$. The saturation parameter is $Q^*=1$.

As in Ref. [29], we will characterize the stationary probability of the population size $Q(t)$ for different values of the delay T and noise parameters. One of the most interesting aspects to analyze are the effect of the non-Gaussian properties of the driving noise.

In Ref. [43], by analyzing a generalized Langevin equation, Eq. (1), with an exponential memory function

$$\Phi(t) = \delta \exp[-\lambda t], \qquad (63)$$

and driven by a symmetrical white shot noise, we have found that the stationary state $P(u)$ develops strong non-Gaussian characteristics only when the rate of the arriving pulses of the noise is smaller than the characteristic decay rate of the corresponding Green function. This condition works both for the monotonous and oscillating regime of the Green function. On the other hand, the amplitude A of the shot noise, introduces only a rescaling of the stationary distribution. We expect that these results remain approximately valid in the present case. In fact, as we will see, after the first period of time T, the delay Green function of Eq. (55) has a decay behavior very similar to that obtained with an exponential kernel.

In Fig. 6 we show a set of stationary distributions $P(Q)$ obtained for different delay times T and maintaining the noise parameters fixed. The noise parameters are $A=0.1$ and $\rho=50$, which implies $D=1$. The parameters of the Green function, Eq. (40), were chosen as $a=0$, and $b=-\pi/2$. The different plots correspond to $T=1/4$ (dotted line), $T=1/2$ (dashed line), and $T=0.85$ (full line). In inset (a) we show the decay behavior of the corresponding delay Green functions. We have tested that after the first interval T, these Green functions can be analytically approximated by the expression
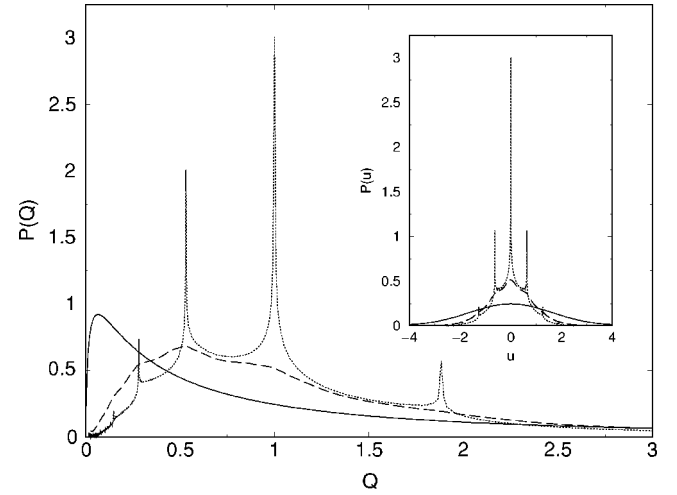
FIG. 7. Stationary distribution $P(Q)$ of the Gompertz model driven by a symmetrical white shot noise for different delay times, $T=0.25$ (dotted line), $T=0.5$ (dashed line), and $T=0.85$ (full line), in all cases taking $b=-\pi/2$. In the inset we show the associated distributions $P(u)$. The noise parameters are $\rho=5/4$ and $A=\sqrt{2/5}$. The saturation parameter is $Q^*=1$.

$$\Lambda(t) = A_0 \exp[-\gamma_0(t-T)]\cos[w_0 t - \phi_0], \quad t > T. \quad (64)$$

For $T=1/4$ we get $\gamma_0=2.6$, $w_0=0$, $\phi_0=0$. For $T=1/2$ we get $\gamma_0=1$, $w_0=2.4$, $\phi_0=1.2$. and for $T=0.85$ we get $\gamma_0=0.143$, $w_0=1.75$, $\phi_0=0.967$. Then, using our previous argument we expect a Gaussian induced behavior (approximately) for $\rho > \gamma_0$. In this figure this condition is clearly satisfied, and the distributions $P(Q)$ can be associated with a Gaussian distribution for the underlying process $u(t)$. In inset (b) we show the corresponding stationary distributions of the process $u(t)$, which in fact, can be very well approximated by Gaussian distributions. Furthermore, we notice that the equilibrium distributions $P(Q)$ coincide with those obtained in Ref. [29] by using a driving Gaussian white noise.

In Fig. 7 the noise parameters are $\rho=5/4$ and $A=\sqrt{2/5}$, which implies $D=1$. Here, as the rate of the noise is smaller than in the previous case, non-Gaussian characteristics for the process $u(t)$ are manifest in the stationary distribution $P(Q)$. In fact, we note that when the decay rate of the Green function is larger than the noise rate ρ, a series of sharp narrow peaks appear in the stationary distribution. This effect is more pronounced for smaller values of T, which in the present example implies bigger values of the characteristic decay rate γ_0.

We notice that the peaks of the stationary distribution $P(Q)$ appear at positions $Q_p=Q^*\exp[\pm pA]$, where p is an arbitrary natural number. This result follows from the fact that in the distribution of the associated process $u(t)$, the peaks appear at positions $u_p=\pm pA$ [43]. This effect can be clearly seen in inset (b), where we have plotted the associated distributions $P(u)$.

In Fig. 8 we show a set of stationary distributions $P(Q)$ by maintaining fixed the time delay $T=0.85$ [$a=0$, $b=-\pi/2$] and changing the noise parameters, $\rho=0.1$ (dotted line), $\rho=0.15$ (dashed line), and $\rho=0.25$ (full line), in all cases
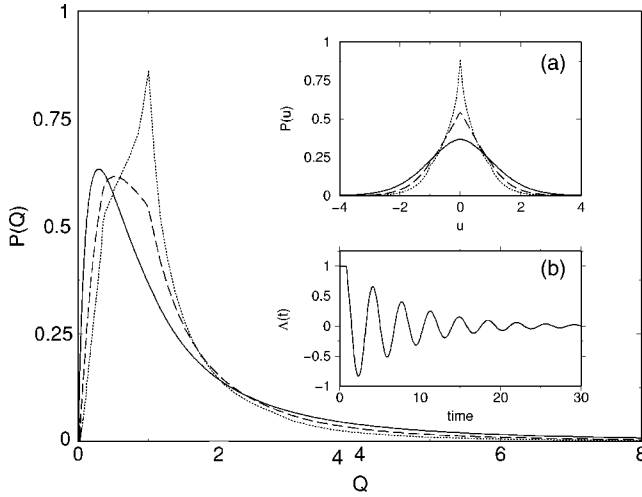
FIG. 8. Stationary distribution $P(Q)$ of the Gompertz model driven by a symmetrical white shot noise for different noise parameters, $\rho=0.1$ (dotted line), $\rho=0.15$ (dashed line), and $\rho=0.25$ (full line), in all cases taking $A=1$. In inset (a) we show the associated distributions $P(u)$. The parameters of the Green function, inset (b), are $T=0.85$ and $b=-\pi/2$. The saturation parameter is $Q^*=1$.
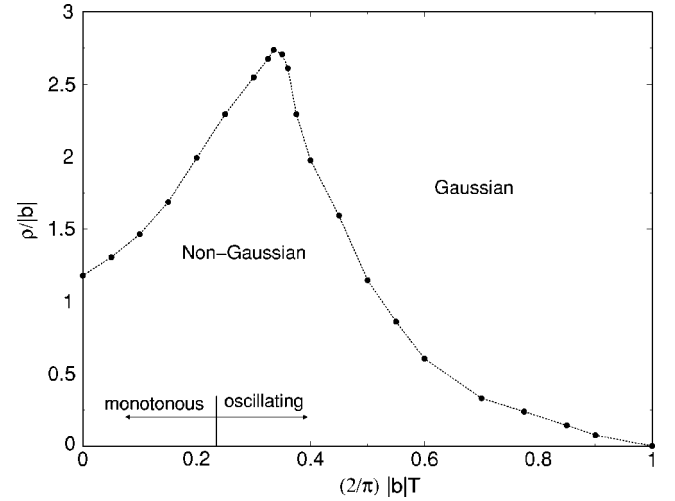

FIG. 9. Phase space of the stationary distribution of the Gompertz model. The curve divides the different regions where the underlying process $u(t)$ develops Gaussian and non-Gaussian characteristics. The circles correspond to the point obtained numerically (see text). The vertical lines indicate the point, on the $(2/\pi)|b|T$ axis, where the Green function changes its characteristic behavior from a monotonous decay to an oscillatory decay.

taking $A=1$. Here the characteristic decay rate of the Green function is $\gamma_0=0.143$. Consistently, we found that non-Gaussian induced aspects tend to arise when $\rho<\gamma_0$. In contrast with the previous figure, here only one peak is visible. In inset (a) we show the associated distributions $P(u)$, where the transition between Gaussian and non-Gaussian distributions is clearly seen.

An important aspect to analyze is the set of values in the space of the parameters A, ρ, b, and T where the stationary distribution $P(Q)$ and the associated distribution $P(u)$ reflect the non-Gaussian structure of the driven noise. As mentioned previously, this problem is determined mainly by the relations between the decay rate of the Green function and the rate ρ of the driving Poisson noise. Furthermore, we notice that the influence of the constant b can always be taken into account by a time rescaling $\tau=|b|t$. On the other hand, the shift amplitude $\pm A$ of the arriving pulse only introduces a rescaling of the full process. Thus, the four-dimensional space can be reduced to a two-dimensional space defined by the rescaled parameters ρ/b and bT.

In Fig. 9 we have plotted the phase space structure of the Gompertz model, by showing the region of parameter values, in the region of stability $-\pi/2<bT<0$, where the stationary distributions depart from those obtained with a driving Gaussian white noise. In order to determine the points that define the boundary line, for each set of parameter values, we have approximated the associated distributions $P(u)$, in an arbitrary interval around the origin $u \in (0,\varepsilon)$, by a quadratic polynomial $P(u) \approx \alpha u^2 + \beta u + P(0)$. Then, it is simple to demonstrate that when $|\alpha\varepsilon/\beta|<1$, the stationary distribution around the origin is dominated by a linear approximation. In this case, $P(u)$ strongly departs from a Gaussian distribution which are characterized by a null slope around the origin. The change of behavior of the slope around the origin can be clearly seen in the insets of Figs. 7 and 8. Furthermore, we have checked that when the condition $|\alpha\varepsilon/\beta|>1$ is satisfied,

the quotient between the fourth cumulant and the square of the second cumulant of the distributions is less than one, indicating that a Gaussian is approaching. We remark that by satisfying only this last condition, it is not possible to guarantee the validity of a Gaussian approximation.

We have checked that the line that divides the two regimes corresponds approximately to the points for which the characteristic decay rate of the delay Green function is of the same order as the rate of the arriving pulses, i.e., $\rho \approx \gamma_0$. In fact, note that in the limit $|b|T\to 0$ the boundary curve goes approximately to $\rho/|b| \approx 1$. This limit corresponds to the nondelay case $T=0$, where $\Lambda(t)=\exp(bt)$. Thus, the non-Gaussian effect appears for $\rho < \gamma_0 \approx |b|$. Furthermore, the behavior near this point can be understood by noting that for small values of bT, the Green function of Eq. (55) can be approximated by $\Lambda(t) \approx \exp[bt/(1+bT)]$. This result implies a local increasing of the characteristic decay rate of the Green function with respect to the case $T=0$. Therefore, the boundary line has a positive slope near $T=0$.

On the other hand, in the limit $(2/\pi)|b|T\to 1$ the Green function oscillates without any decay. Thus, its characteristic decay rate γ_0 goes to zero, which implies that in this limit the dynamics does not develop any non-Gaussian characteristic. Near the point $(2/\pi)|b|T=1$, the Green function presents a non-null decay rate whose value increases by diminishing T.

At intermediate values of $(2/\pi)|b|T$ the Gaussian-non-Gaussian boundary line reach a maximum value. Clearly, this effect arise due to the different dependences of the decay rate of the Green function near the boundary of stability, $(2/\pi)|b|T\approx 0$ and $(2/\pi)|b|T\approx 1$.

In this plot, we have indicated with a vertical line the value $|b|T=1/e$, which corresponds to the point where the Green function of Eq. (55) changes its characteristic behavior from a monotonous decay to an oscillatory one [27]. As

can be seen from the plot, the kind of decay of the Green function does not have any influence in the phase space of the parameters.

Finally, we want to comment on the difference among the *non-Gaussian properties* of the stationary distributions obtained by choosing either an exponential kernel, Eq. (63), or the delay kernel, Eq. (19) [$a=0$]. As was touched on previously, the main difference between the behaviors of the corresponding Green functions appears in the first interval of time T, where the delay Green function is constant, $\Lambda(t)=1$. This property implies the absence of any dissipation in the time interval $0<t<T$. In consequence, the non-Gaussian peaks of the delay distributions are much higher that in the case of the exponential kernel. In fact, in absence of dissipation the realizations of the process $u(t)$ consist in a discrete random walk over the sites $u_p=\pm pA$. Clearly, this enhanced effect is more pronounced when the delay time T is of the order of the characteristic time decay of the Green function $\Lambda(t)$.

V. SUMMARY AND CONCLUSIONS

We have presented a functional formalism that allows a full characterization of linear delay Langevin equations with arbitrary external fluctuations defined through its characteristic functional. This method relies on the possibility of obtaining an explicit expression for the realizations of the delay stochastic process in terms of the associated Green function of the linear problem. Then, the characteristic functional of the delay process can be written in terms of that of the noise and in terms of the delay Green function. From the characteristic functional it is possible to get any n-joint probability density and any n-time moment or cumulant.

By analyzing the dissipative transient dynamics over the boundaries of stability, we have found some amazing and interesting characteristic behaviors. First, when the dissipative constants are much larger than the inverse of the delay time $1/T$, the transient dynamics presents a kind of periodic *closedness* to the external perturbations. In this situation, the system only responds to the external world within small windows of time. On the other hand, over both boundary lines, in the long time regime, the Green function develops a *quasistationary state* where it decays in an exponential way with a rate much larger than the characteristic rate constants of the dissipative dynamics. Over the parametric boundary line, Eqs. (46) and (47), the decay is oscillatory and over the boundary line $a=b$ the decay is monotonous.

As a concrete application of our formalism we have analyzed the Gompertz model of population growth driven by a symmetric white shot noise. This model can be mapped with a linear delay Langevin equation, where our formalism applies. We have shown that the non-Gaussian property of this noise may lead to the occurrence of narrow peaks in the stationary population distribution. This striking property is directly related to the possibility of obtaining non-Gaussian stationary distributions in the associated linear delay Langevin equation. This last property arises when the average waiting-time between the arrival of the δ-Dirac pulse of the white shot noise is larger than the characteristic decay time of the delay Green function.

Finally, we want to remark that our formalism opens the possibility of studying linear delay process driven by arbitrary noises, such as radioactive noise, Levy noise, and Abel noise [43]. In the last two cases, both noises may induce long-tail structures in the population distributions.

[1] N. G. van Kampen, in *Stochastic Processes in Physics and Chemistry*, 2nd. ed. (North-Holland, Amsterdam, 1992).

[2] M. O. Cáceres *Elementos de Estadistica de no Equilibrio y sus Aplicaciones al Transporte en Medios Desordenados* (Reverté S.A., Barcelona, 2003).

[3] R. Kubo, Rep. Prog. Phys. **29**, 255 (1966).

[4] R. Zwanzig, in *Lectures in Theoretical Physics*, Boulder, Vol. III, edited by W. E. Broton (Interscience, New York, 1961).

[5] H. Mori, Phys. Rev. **112**, 1829 (1958).

[6] H. Grabert, *Projection Operator Techniques in Nonequilibrium Statistical Mechanics*, Vol. 95 of Springer Tracts in Modern Physics (Springer-Verlag, Berlin, 1982).

[7] S. Chatuverdi and F. Shibata, Z. Phys. B **35**, 297 (1979).

[8] K. Ikeda, H. Daido, and O. Akimoto, Phys. Rev. Lett. **45**, 709 (1980).

[9] P. Nardone, P. Mandel, and R. Kapral, Phys. Rev. A **33**, 2465 (1986).

[10] C. M. Marcus and R. M. Westervelt, Phys. Rev. A **39**, 347 (1989).

[11] A. Longtin, J. G. Milton, J. E. Bos, and M. C. Mackey, Phys. Rev. A **41**, 6992 (1990).

[12] A. Longtin, Phys. Rev. A **44**, 4801 (1991).

[13] P. Tass, J. Kurths, M. G. Rosenblum, G. Guasti, and H. Hefter, Phys. Rev. E **54**, R2224 (1996).

[14] Y. Chen, M. Ding, and J. A. Scott Kelso, Phys. Rev. Lett. **79**, 4501 (1997).

[15] S. Kim, S. H. Park, and H.-B. Pyo, Phys. Rev. Lett. **82**, 1620 (1999).

[16] L. S. Tsimring and A. Pikovsky, Phys. Rev. Lett. **87**, 250602 (2001).

[17] C. Masoller, Phys. Rev. Lett. **86**, 2782 (2001).

[18] C. Masoller, Phys. Rev. Lett. **90**, 020601 (2003).

[19] R. D. Driver, *Ordinary and Delay Differential Equations* (Springer-Verlag, Berlin, 1977).

[20] J. K. Hale and S. M. Verduyn Lunel, *Introduction to Functional Differential Equations* (Springer-Verlag, Berlin, 1993).

[21] U. Kuechler and B. Mensch, Stoch. Stoch. Rep. **40**, 23 (1992).

[22] T. Ohira and J. G. Milton, Phys. Rev. E **52**, 3277 (1995).

[23] T. Ohira, Phys. Rev. E **55**, R1255 (1997).

[24] T. Ohira and Y. Sato, Phys. Rev. Lett. **82**, 2811 (1999).

[25] T. Ohira and T. Yamane, Phys. Rev. E **61**, 1247 (2000).

[26] M. C. Mackey and I. G. Nechaeva, Phys. Rev. E **52**, 3366 (1995).

[27] S. Guillouzic, I. L'Heureux, and A. Longtin, Phys. Rev. E **59**, 3970 (1999).

[28] S. Guillouzic, I. L'Heureux, and A. Longtin, Phys. Rev. E **61**,

4906 (2000).

[29] T. D. Frank and P. J. Beek, Phys. Rev. E **64**, 021917 (2001).

[30] T. D. Frank, Phys. Rev. E **66**, 011914 (2002).

[31] T. D. Frank, P. J. Beek, and R. Friedrich, Phys. Rev. E **68**, 021912 (2003).

[32] J. Heinrichs, Phys. Rev. E **47**, 3007 (1993).

[33] A. Fulinski, Phys. Rev. E **50**, 2668 (1994).

[34] A. Drory, Phys. Rev. E **51**, 5298 (1995).

[35] J. Masoliver and K. G. Wang, Phys. Rev. E **51**, 2987 (1995).

[36] J. M. Porra, K. G. Wang, and J. Masoliver, Phys. Rev. E **53**, 5872 (1996).

[37] S. I. Denisov and W. Horsthemke, Phys. Rev. E **62**, 7729 (2000).

[38] T. Srokowski, Phys. Rev. Lett. **85**, 2232 (2000).

[39] T. Srokowski, Phys. Rev. E **64**, 031102 (2001).

[40] R. Morgado, F. Oliveira, G. G. Batrouni, and A. Hansen, Phys. Rev. Lett. **89**, 100601 (2002).

[41] M. O. Cáceres and A. A. Budini, J. Phys. A **30**, 8427 (1997).

[42] A. A. Budini and M. O. Cáceres, J. Phys. A **32**, 4005 (1999).

[43] A. A. Budini and M. O. Cáceres, J. Phys. A **37**, 5959 (2004).

[44] M. O. Vlad, J. Ross, and M. C. Mackey, J. Math. Phys. **37**, 803 (1996).

[45] M. O. Vlad, J. Ross, and F. W. Schneider, Phys. Rev. E **62**, 1743 (2000).

[46] M. O. Vlad, F. W. Schneider, and J. Ross, Physica A **294**, 1 (2001).